Assignment I

EE4725 Quasi Optical Systems

Petar V. Peshev, p.v.peshev@student.tudelft.nl
Department of Electrical Engineering, Mathematics, and Computer Science,
Delft University of Technology, Delft, The Netherlands

I. Elementary Electric Source

The real and imaginary part of the xx-component of the free space Spectral Green's Function (SGF), for a frequency $f = 28$ GHz, as a function of the normalized wave vector's x-component, to the free space propagation constant, is plotted in Fig.1.

The real and imaginary part of the SGF's yy-component for $f = 28$ GHz as a function of the normalized wave vector's x-component, to the free space propagation constant, is plotted in Fig.2.

The z-componnet of the wave vector is

$$k_z = \sqrt{k^2 - k_x^2 - k_y^2}, \tag{1}$$

As the x-component of the wave vector approaches the magnitude of the propagation constant, the z-component of the propagation constant becomes imaginary. Hence, the XX and YY-components of the SGF are real when the wave vector's x-component is lower than the propagation constant $k_x < k_0$, and imaginary when $k_x > k_0$.

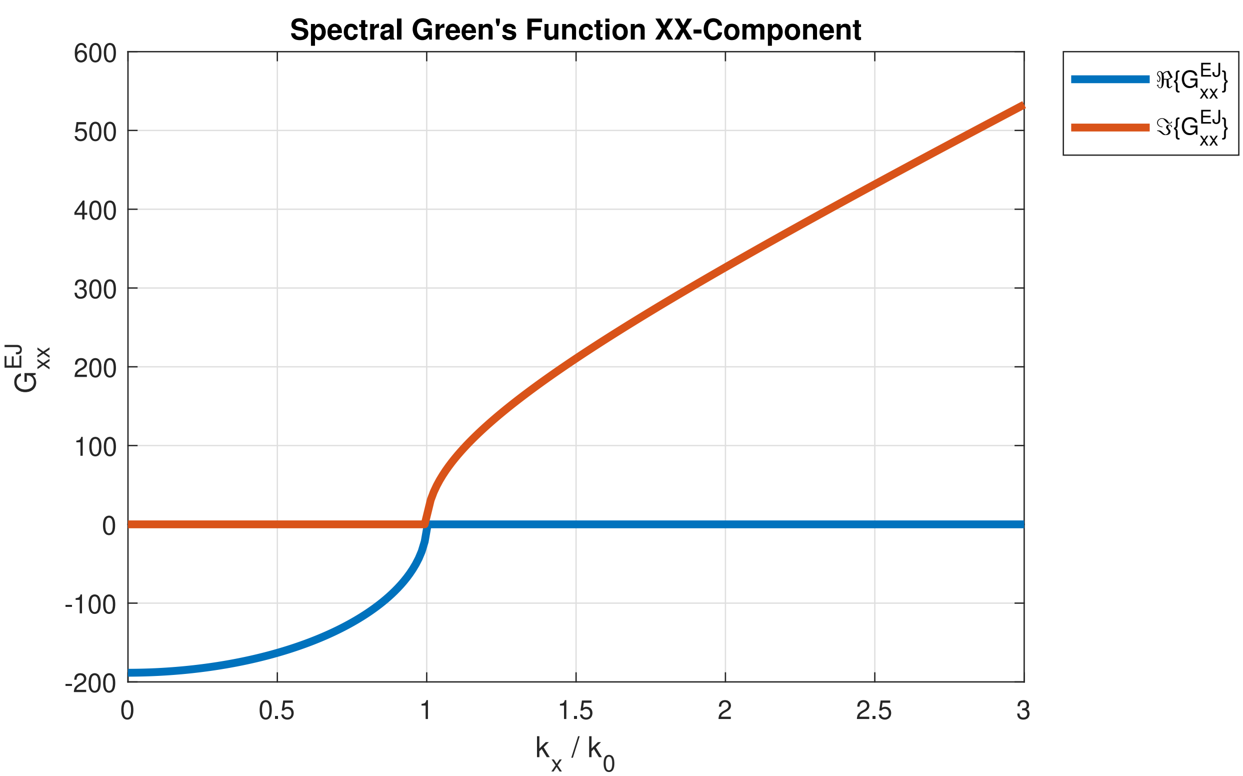

Fig. 1. Real and imaginary parts, in blue and red respectively, of the free space Spectral Green's Function's xx-component, as a function of normalized wave vector's x-component to the free space propagation constant, for frequency $f = 28$ GHz, and wave vector's x and y-components $k_x \in [0, 3k_0]$ and $k_y = 0$ for points respectively.

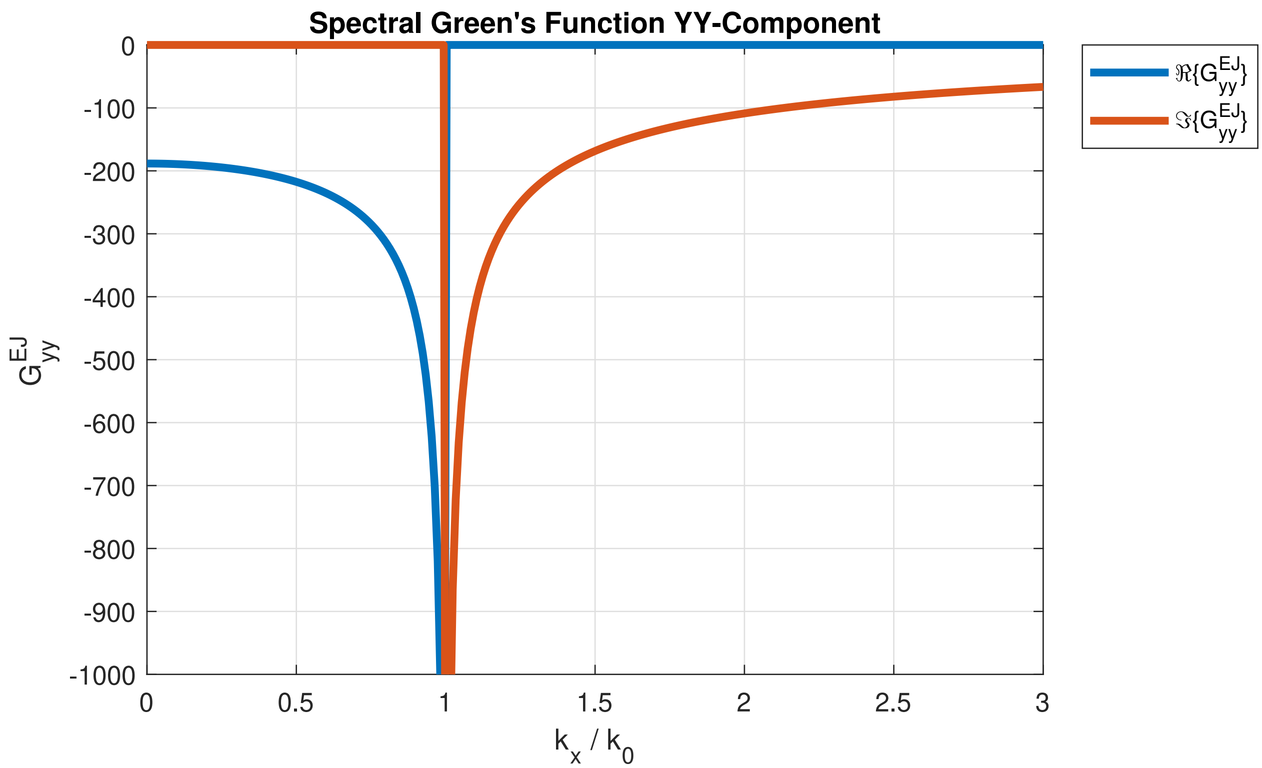

Fig. 2. Real and imaginary parts, in blue and red respectively, of the free space Spectral Green's Function's yy-component, as a function of normalized wave vector x-component to the free space propagation constant, for frequency $f = 28\ GHz$, and wave vector's x and y-components $k_x \in [0, 3k_0]$ and $k_y = 0$ for points respectively.

II. Far-Field of a Dipole

The dipole has a length $L = \lambda_0/2$ and width $W = \lambda_0/40$, where λ_0 is the free space wavelength, and is oriented along the x-axis; the frequency of operation is $f = 28\ GHz$.

The total electric far-field in the planes $\phi = 0°, 45°, 90°$ of the dipole is plotted in Fig.3. Furthermore, the UV representation of the E far-field, in $(37.5, 30)$ and top views, are plotted in Fig.4 and Fig.5 respectively. The radiation pattern of a dipole is a horn torus with center oriented along the dipole; hence, there is no radiation along the orientation of the dipole (x-axis) and maximum radiation perpendicular to the dipole. Consequently, as a a result of the dipole's orientation, the total electric field is constant at $\phi = 90°$, and does not radiate at $\theta = 90°, \phi = 0°$. Moreover, due to the horn torus shape, the E far-field is uniform with respect to the V-coordinate in the UV-representation.

The dipole's broadside's directivity ($\theta = 0°$ and $\phi = 0°$) as a function of the frequency is plotted in Fig.6. As a consequence of

$$\vec{J}_{FT}(k_x, k_y) = \frac{2k_{eq}(\cos(\frac{k_x l}{2}) - \cos(\frac{k_{eq} l}{2}))}{(k_{eq}^2 - k_x^2)\sin(k_{eq}\frac{l}{2})} sinc(\frac{k_y w}{2})\hat{x}, \tag{2}$$

the radiation pattern of the dipole actually changes as the product between the propagation constant and dipole's length changes. As this product increases, the radiation pattern oscillates between a horn torus and a pattern with a minimum at the broadside and four beams offset at $\pm 45°$ and $\pm 135°$ from broadside. This effect results in no broadside radiation at frequencies with dipole length to wavelength ratio of approximately multiple of 2, observed on Fig.6.

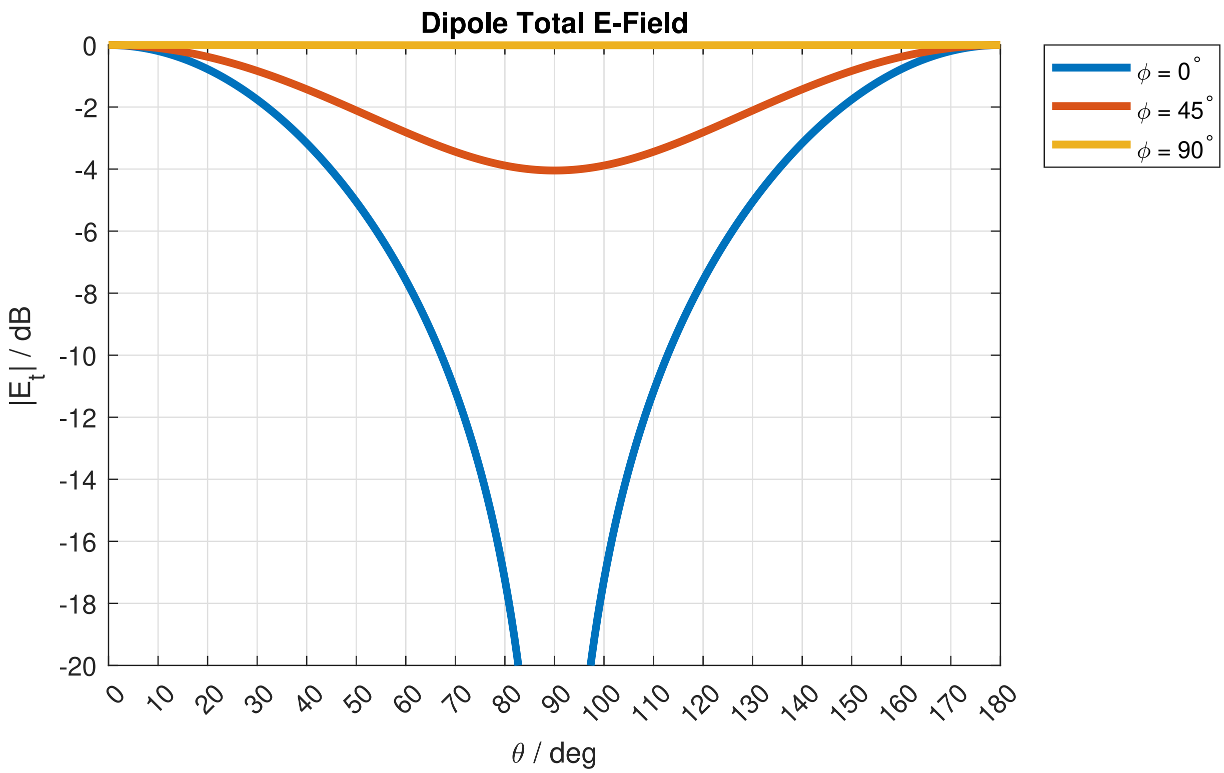

Fig. 3. Total electric far-field in free space in dB, in the planes $\phi = 0°, 45°, 90°$, for frequency $f = 28\ GHz$ of a dipole oriented along the x-axis, length and width $L = \lambda_0/2$ and $W = \lambda_0/40$ respectively (where λ_0 is the free space wavelength).

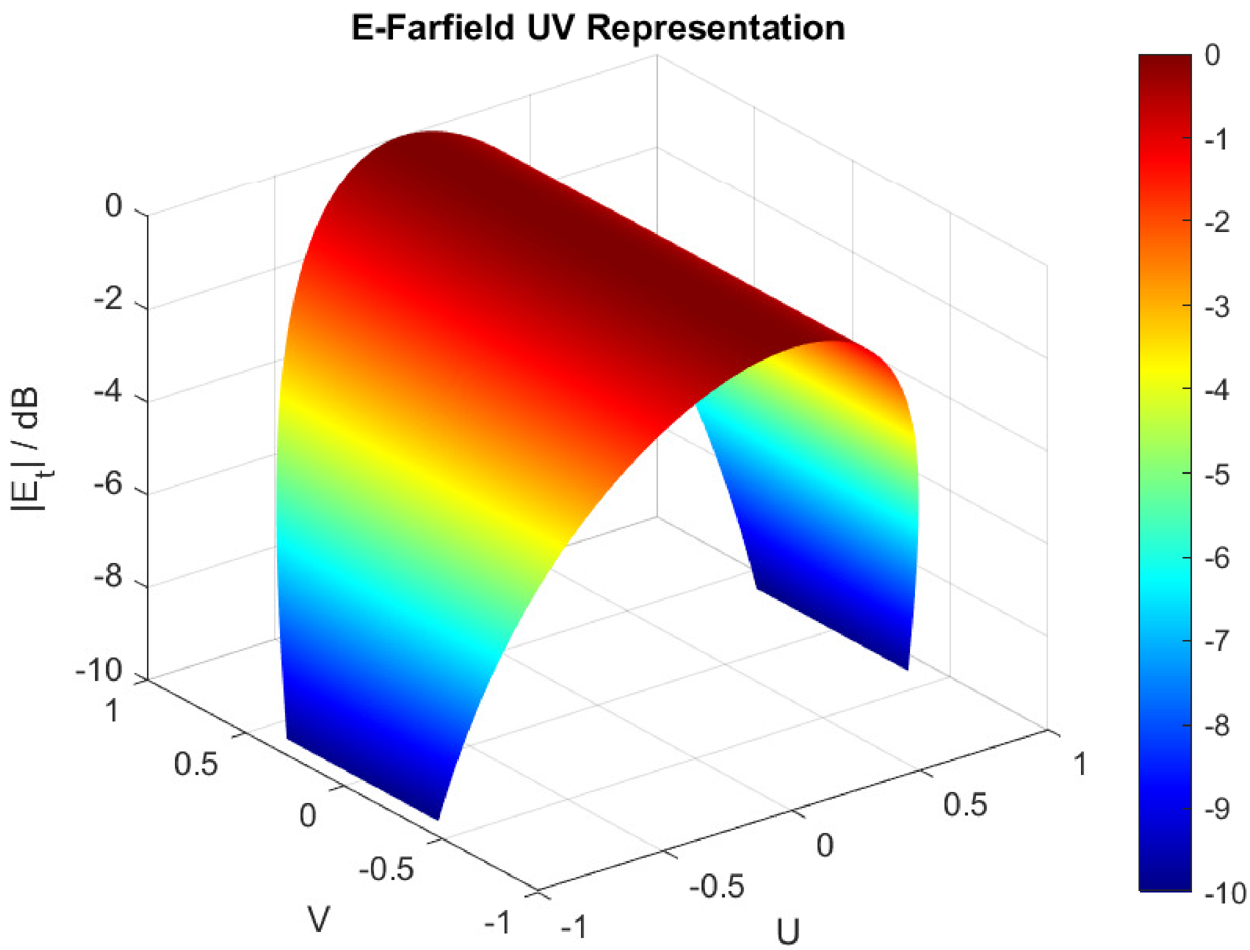

Fig. 4. UV representation, view $(37.5, 30)$, of total electric far-field in free space, in upper medium $z > 0$, for frequency $f = 28\ GHz$ of a dipole oriented along the x-axis, length $L = \lambda_0/2$, and width $W = \lambda_0/40$ (where λ_0 is the free space wavelength).

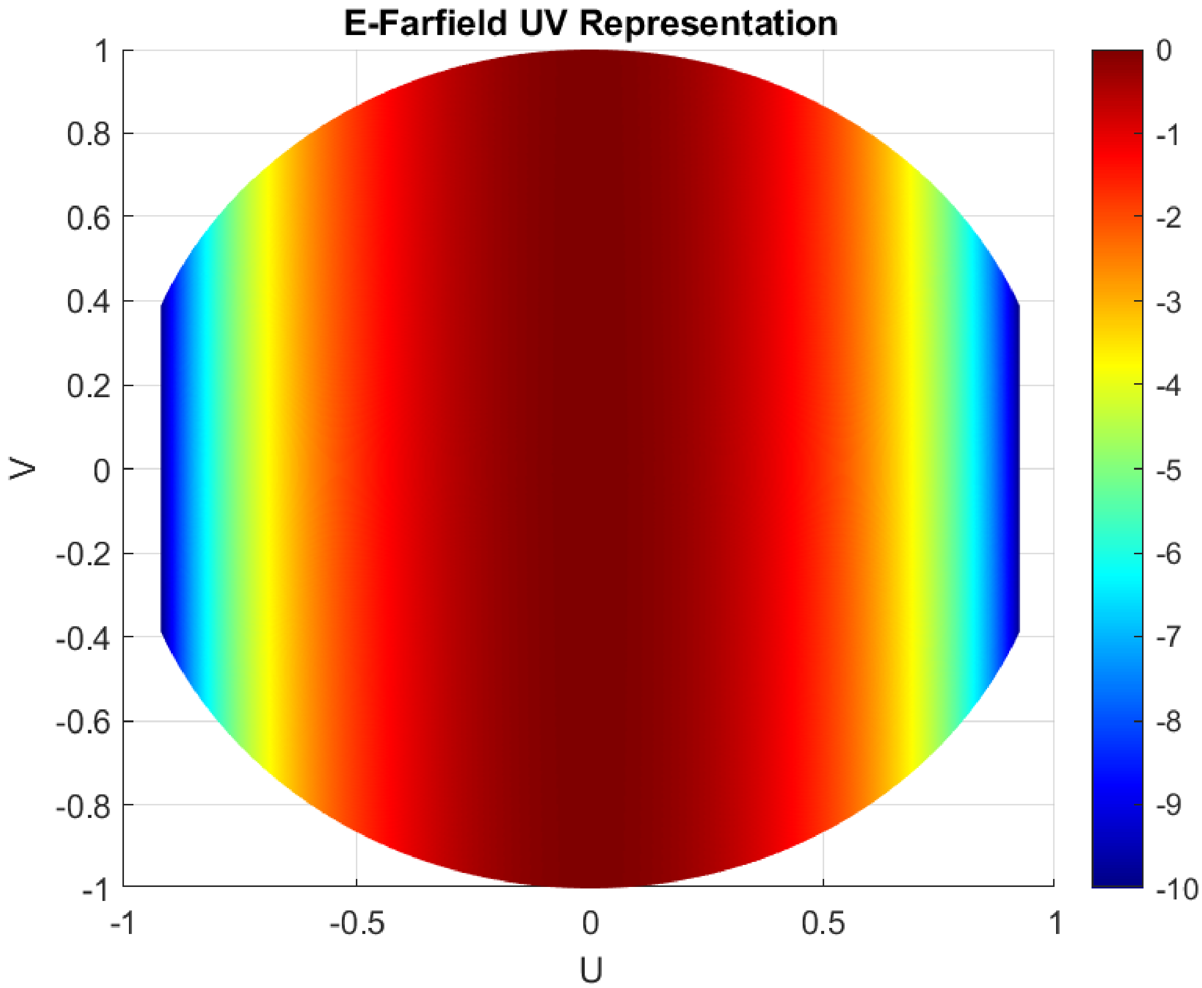

Fig. 5. Top view UV representation of total electric far-field in free space, in upper medium $z > 0$, for frequency $f = 28\ GHz$ of a dipole oriented along the x-axis, length $L = \lambda_0/2$, and width $W = \lambda_0/40$ (where λ_0 is the free space wavelength).

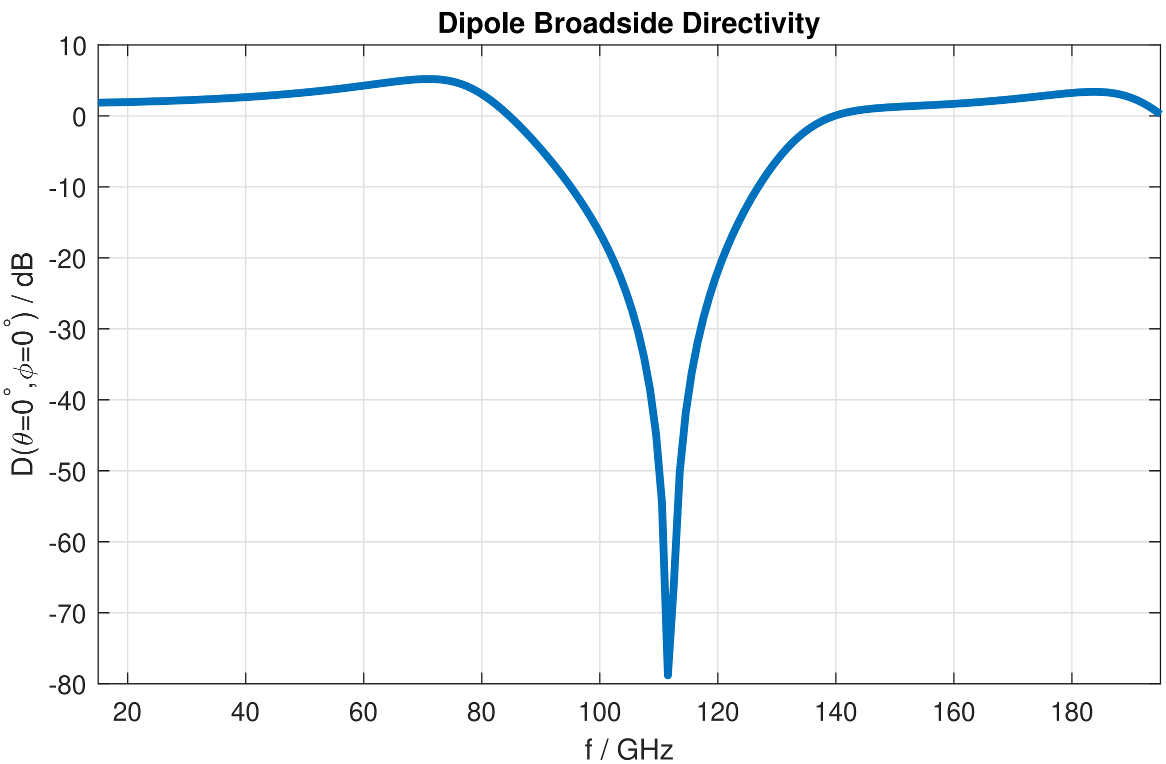

Fig. 6. Broadside ($\theta = 0°$ and $\phi = 0°$) directivity in dB as a function of the frequency f of a dipole oriented along the x-axis, length $L = \lambda_0/2$, and width $W = \lambda_0/40$ (where λ_0 is the free space wavelength).

III. Dipole With Backing Reflector

The dipole has the same orientation and dimensions at the same frequency of operation as the dipole in Section.II, however, a backing reflector is placed at $h = 5.36\ mm$ under it.

The total electric far-field in the planes $\phi = 0°, 45°, 90°$ of the dipole with backing reflector is plotted in Fig.7. Furthermore, the UV representation of the E far-field, in $(37.5, 30)$ and top views, are plotted in Fig.8 and Fig.9 respectively. As the wave is reflected at the metal interface, the in-phase reflected and direct waves create zones of radiation, while the out-of-phase waves create zones of no radiation. Consequently, beams form up in these zones of radiation. Moreover, the beam at broadside ($\theta = 0°$ and $\phi = 0°$) is dependent on the reflector-dipole spacing; in case the spacing is a multiple of quarter of the wavelength, the direct and reflected waves at broadside are in-phase, resulting in maximum directivity; on the other hand, in case the spacing is a multiple of half of the wavelength, the waves are out-of-phase, resulting in minimum directivity. As the spacing goes from a multiple of the quarter to half of the wavelength, the side-beams' beamwidth becomes larger, however, their locations do not change. For the considered dipole-reflector spacing of $h = 5.36\ mm$, h is a multiple of the half of the wavelength, consequently no main / broadside beam is observed and the beamwidth of the side-lobes is at maximum. This effect is observed on the UV representations in Fig.8 and Fig.9.

The dipole's broadside directivity ($\theta = 0°$ and $\phi = 0°$) as a function of the dipole-reflector spacing is plotted in Fig.10. As previously mentioned the broadside directivity oscillates as the dipole-reflector spacing goes from quarter to half of the wavelength. This conclusion is observed on Fig.10, where as h increases, the directivity oscillates between maximum and minimum, due to the in-phase and out-of-phase direct and reflected waves respectively.

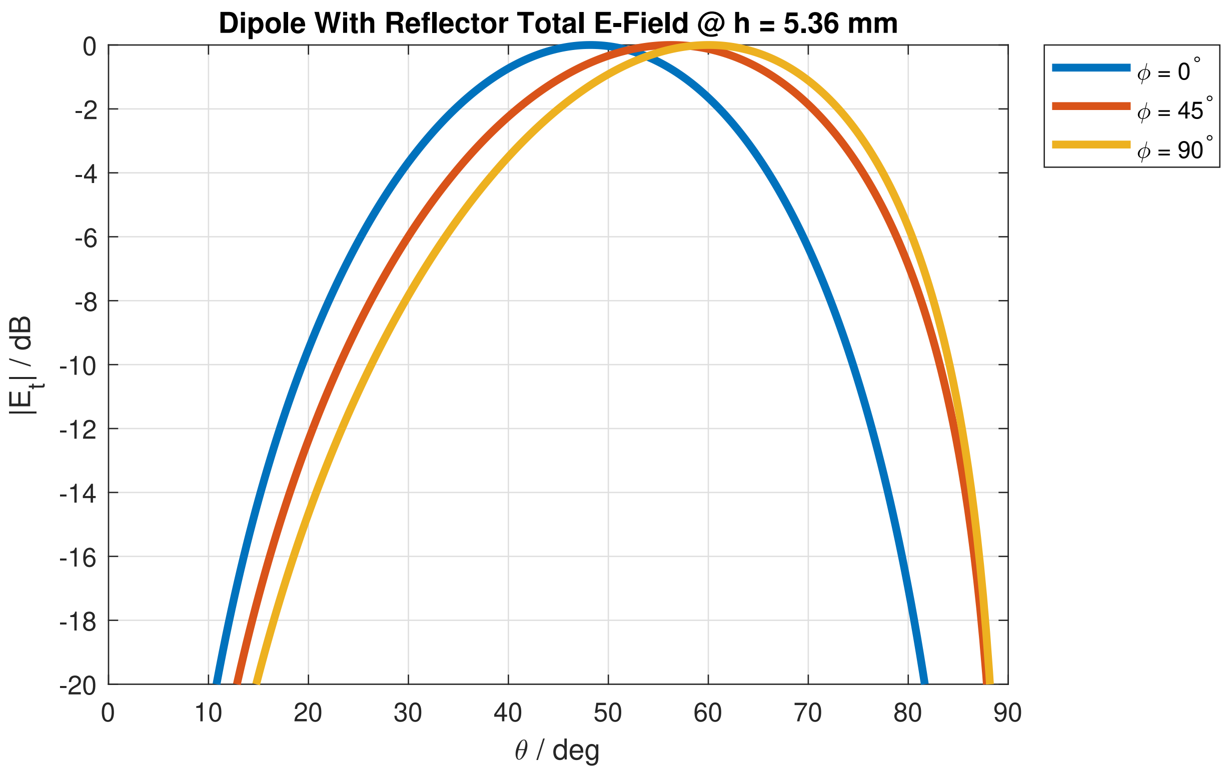

Fig. 7. Total electric far-field in free space in dB, in the planes $\phi = 0°, 45°, 90°$, for frequency $f = 28\ GHz$ of a dipole with backing reflector, at distance $h = 5.36\ mm$, oriented along the x-axis, length and width $L = \lambda_0/2$ and $W = \lambda_0/40$ respectively (where λ_0 is the free space wavelength).

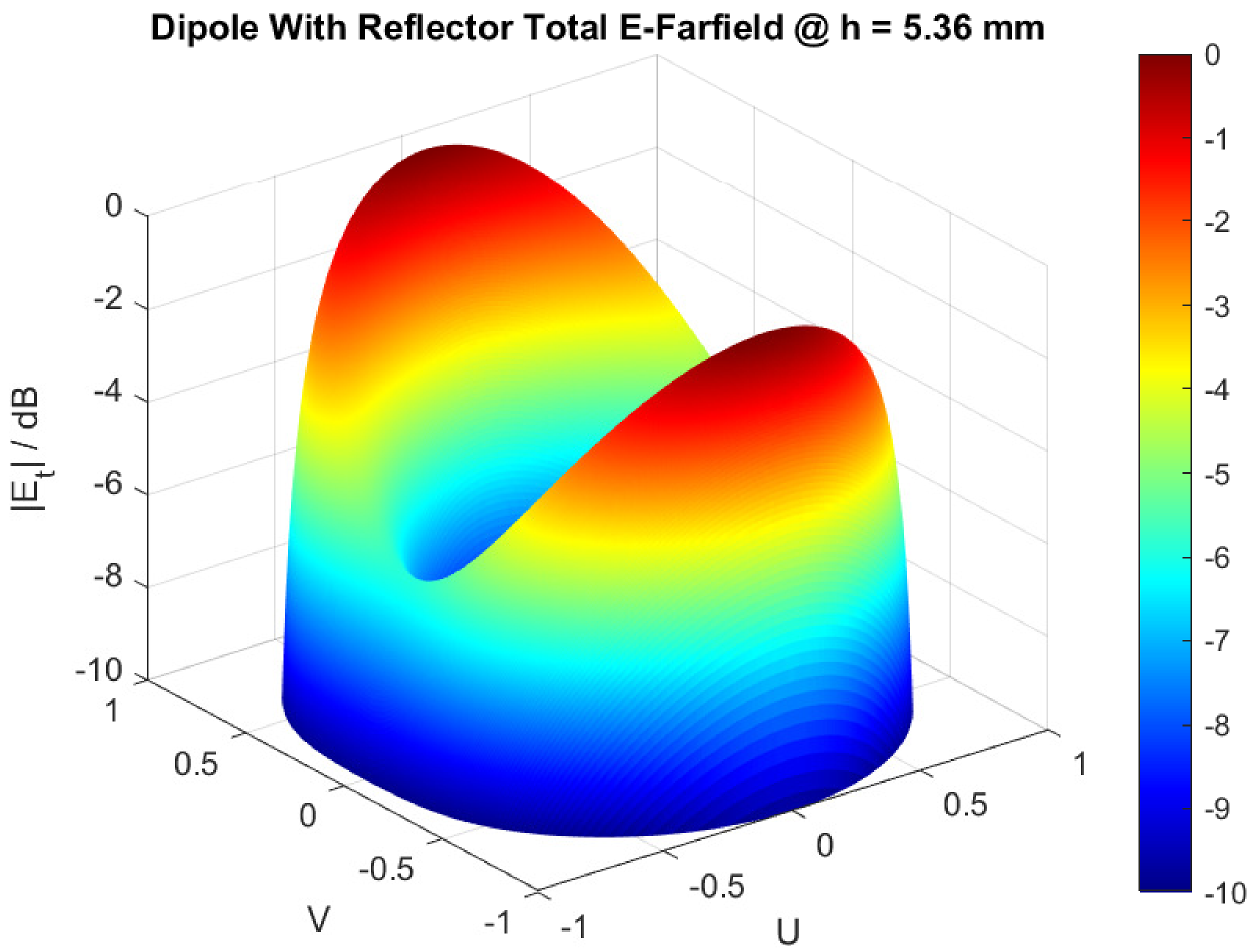

Fig. 8. UV representation, view $(37.5, 30)$, of total electric far-field in free space, in upper medium $z > 0$, for frequency $f = 28\ GHz$ of a dipole with backing reflector, at distance $h = 5.36\ mm$, oriented along the x-axis, length $L = \lambda_0/2$, and width $W = \lambda_0/40$ (where λ_0 is the free space wavelength).

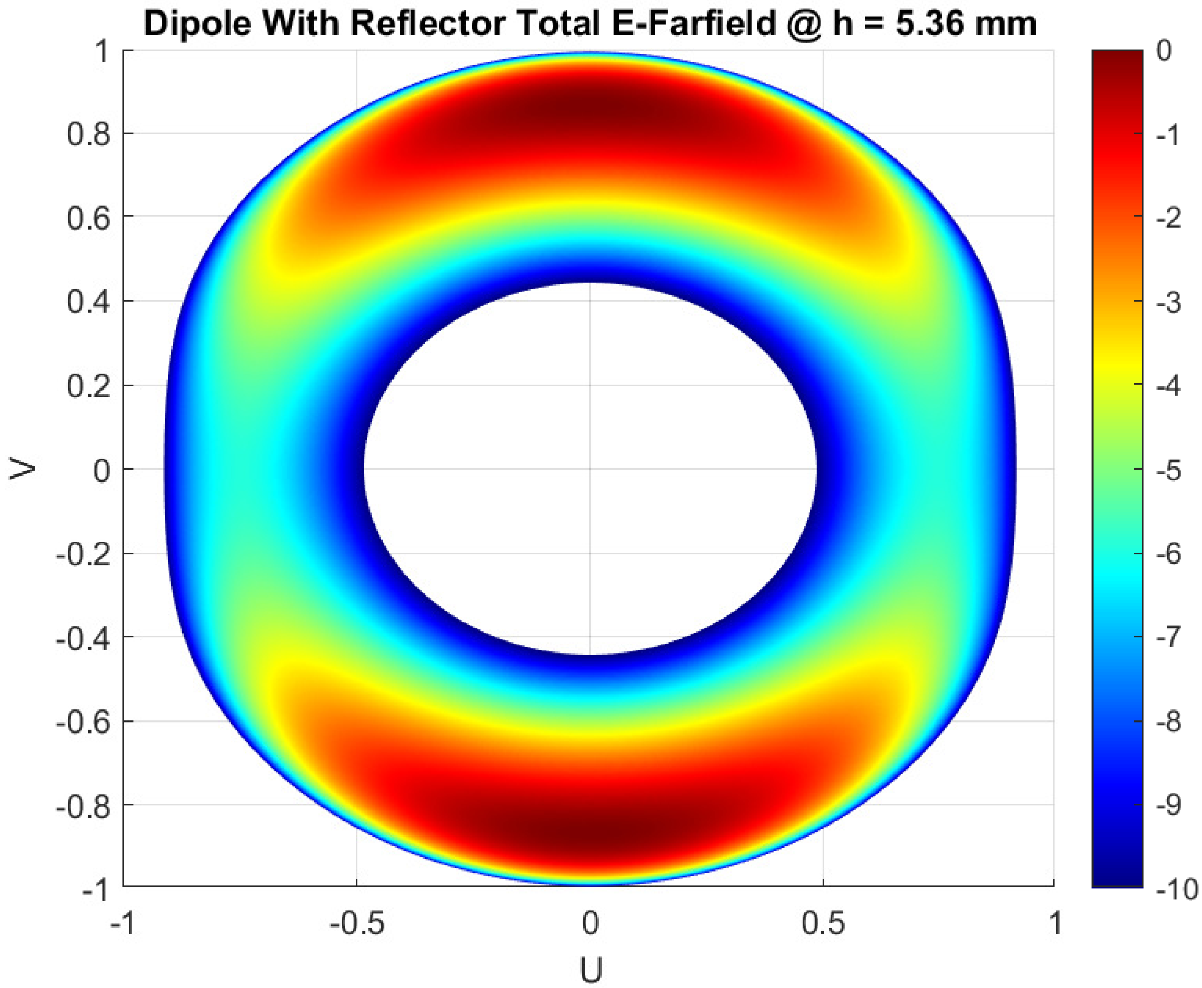

Fig. 9. Top view UV representation of total electric far-field in free space, in upper medium $z > 0$, for frequency $f = 28\ GHz$ of a dipole with backing reflector, at distance $h = 5.36\ mm$, oriented along the x-axis, length $L = \lambda_0/2$, and width $W = \lambda_0/40$ (where λ_0 is the free space wavelength).

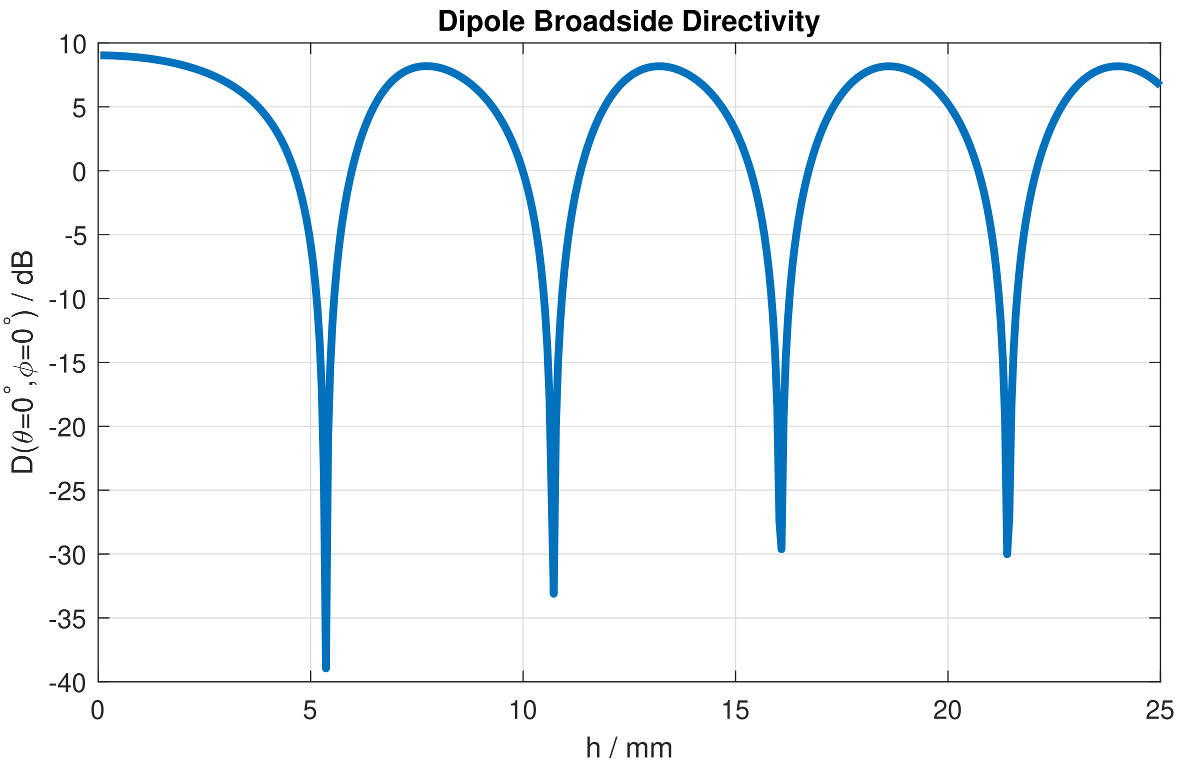

Fig. 10. Broadside ($\theta = 0°$ and $\phi = 0°$) directivity in dB as a function of the dipole-reflector spacing h, for $f = 28\ GHz$, of a dipole with backing reflector oriented along the x-axis, length $L = \lambda_0/2$, and width $W = \lambda_0/40$ (where λ_0 is the free space wavelength).

Appendix

The solutions of the assignment are Assignment I Repository, and the library is at quasi-optics-library.